© 2026 IJRTI | Volume 11, Issue 6 June 2026 | ISSN: 2456-3315

Vibration and Explicit Analysis for impact test of a Heavy-Lift Hexacopter Drone

[1]Boda Devender, [2]Dr. K. Gurubrahmam
1M.E. Student (CAD-CAM), 2Assistant Professor
devenderbablu3@gmail.com, gurubrahmam_mech@cbit.ac.in
Department of Mechanical Engineering,
Chaitanya Bharathi Institute of Technology (A), Gandipet, Hyderabad – 500075, Telangana, India

Abstract: Unmanned Aerial Vehicles (UAVs) are increasingly deployed in aerial surveillance, precision agriculture, environmental monitoring, disaster management, logistics and infrastructure inspection. In all of these roles the structural frame governs flight stability, payload capability, vibration resistance and impact durability, so the selection of a lightweight material and the verification of its structural performance are critical to safe operation. This paper presents the design, parametric modelling and finite element analysis (FEA) of a heavy-lift hexacopter (six-rotor) drone frame made of Carbon Fibre Reinforced Polymer (CFRP). A three-dimensional model of the 800 mm-diagonal frame — central hexagonal body, six tubular arms, motor-mounting pads and a landing structure — was developed in SolidWorks 2025 and imported into ANSYS Workbench for simulation, with the frame modelled as an orthotropic Epoxy Carbon UD laminate of total frame-and-motor mass ≈ 1.84 kg. Static structural analysis was carried out at four payload levels (25, 50, 75 and 100 N) on a mesh-independent model of ≈ 1.05 million elements, and the CFRP frame was compared against an identical Nylon 6/6 frame. Modal analysis extracted the first six natural frequencies; harmonic response analysis (0–700 Hz, 100 N) evaluated the steady-state dynamic response; and two explicit-dynamic analyses assessed the landing structure under a gravity-settling case and a 1 m hard-drop impact. The maximum Von-Mises stress rose linearly from 24.0 MPa at 25 N to 96.0 MPa at the critical 100 N load, where the maximum deformation was 1.387 mm and the factor of safety (FoS) was 15.63 — about 10.4× the required minimum of 1.5. At the same load the Nylon 6/6 frame failed (FoS = 0.83). The first six natural frequencies (192.49–687.81 Hz) lie well above the motor-excitation range; the harmonic analysis gave a maximum stress of 85.78 MPa and a deformation of only 0.077 mm. The 1 m drop produced a peak stress of 385.84 MPa against the 1500 MPa CFRP strength (FoS = 3.89). The results establish that the proposed lightweight CFRP hexacopter frame is structurally safe, dynamically stable and impact-resistant, making it well suited to reliable heavy-lift UAV applications.

Index Terms – UAV, Hexacopter Drone, CFRP, Finite Element Analysis, Static Structural Analysis, Modal Analysis, Harmonic Response Analysis, Explicit Dynamic Analysis, ANSYS Workbench, Composite Materials.

I. INTRODUCTION

The study of Unmanned Aerial Vehicles (UAVs) has gained significant traction in modern engineering owing to vast applications in precision agriculture, industrial inspection, disaster management and logistics. Among multi-rotor configurations, the hexacopter — six rotors arranged symmetrically around a central hub — has emerged as the preferred platform for heavy-lift operations because of its superior motor redundancy, payload capacity and structural symmetry. The structural design of the frame is the most critical challenge, since a frame that deforms or fails under payload loading tilts the rotor discs, degrades thrust efficiency and can cause catastrophic loss of the vehicle.

With the increasing demand for compact, lightweight and structurally efficient airframes, Carbon Fibre Reinforced Polymer (CFRP) composites have been adopted for UAV frame construction. CFRP offers exceptional specific stiffness (E/ρ) and specific strength (σ_{UTS}/ρ) while minimising structural mass, enabling higher payload fractions and extended endurance. This work presents the design optimisation and structural FEA validation of a heavy-lift hexacopter frame fabricated from carbon-fibre prepreg.

A hexacopter retains stable controlled flight after the complete failure of any single motor, as the remaining five rotors compensate through differential thrust — a safety capability absent in quadcopters and indispensable for operations over populated areas or critical infrastructure. Six 3510-class motors collectively provide 176.58 N of thrust, enabling 15–20 kg operational payloads, whereas an equivalent quadcopter achieves only 9–10 kg. The symmetric six-point thrust arrangement also produces balanced frame loading and superior yaw authority during precision hover.

The objectives of this study are to: (i) develop a high-fidelity parametric CAD model of an 800 mm-diagonal hexacopter frame; (ii) select the optimal structural material through multi-criteria evaluation; (iii) perform static structural FEA at four payload levels and obtain the Von-Mises stress, total deformation and factor of safety; (iv) verify mesh convergence; (v) perform modal analysis for the first six natural frequencies and mode shapes; (vi) perform harmonic response analysis over 0–700 Hz; and (vii) perform explicit dynamic analysis of the landing structure under impact, validating CFRP against Nylon 6/6 under identical geometry and loading.

II. LITERATURE REVIEW

Raut et al. [1] developed a 3D hexacopter model and performed FEA comparing carbon fibre and ABS for a 3 kg payload, confirming that carbon fibre produces significantly lower deformation and that the arm-hub junction is the primary stress-concentration site. Gutierrez-Rivera et al. [2] designed and experimentally validated a hexacopter for a 30 kg agricultural payload, reporting less than 8% deviation from FEA and showing that arm-hub junctions account for over 65% of peak stress. Srivastav et al. [3] compared tricopter, quadcopter, hexacopter and octocopter frames and identified the hexacopter as offering the optimal balance of payload capacity, redundancy and structural efficiency, with carbon fibre consistently outperforming nylon and aluminium.

In composite-material studies, Vijayalakshmi et al. [6] employed fluid–structure interaction across ~140 material combinations and identified a CFRP/Nomex sandwich as optimal, while Karpenko et al. [7] used a multi-objective genetic algorithm to achieve 18–24% mass reduction without compromising natural frequency. Kubit et al. [8] showed that autoclave curing yields the highest bending strength (1088 MPa), and Li et al. [14] established that autoclave-cured laminates achieve tensile strengths of 1450–1550 MPa at fibre volume fractions of 58–62%, directly validating the orthotropic properties adopted here.

On dynamic behaviour, Chen et al. [10] showed experimentally that dominant arm-vibration frequencies fall below 200 Hz, validating the harmonic sweep range, and Ferretti et al. [12] reported that ply-level (ACP) FEA matched experimental bending frequencies within 8%, far better than the 12–20% error of an isotropic approximation. The review reveals consistent gaps: most studies treat static loading only, comparative CFRP-versus-Nylon studies for the 15–20 kg class are scarce, mesh-independence verification is rarely documented, and integrated harmonic response analysis is largely absent. The present study addresses these gaps through combined static, modal, harmonic and explicit-dynamic FEA with orthotropic CFRP properties.

III. METHODOLOGY

A. CAD Modelling and Frame Geometry

A parametric model of the 800 mm-diagonal frame was developed in SolidWorks 2025 (Fig. 1). The central structural element is a regular hexagonal plate of 200 mm inscribed diameter and 3 mm thickness, whose six-fold symmetry guarantees equal 60° angular spacing of the arms and balanced force paths. Six arm-mounting slots and a twelve-bolt M3 pattern provide the fastening interface, with 1.5 mm fillets at internal corners to avoid stress concentrations.

Fig. 1. SolidWorks CAD assembly of the full hexacopter frame (800 mm diagonal, six rotors).

Each of the six arms is a hollow rectangular tube (400 mm long, 25 × 15 mm section, 2 mm wall). The rectangular section provides a higher second moment of area ($I_x \approx 4702$ mm^4) than an equivalent-mass circular section (≈ 3420 mm^4), yielding ~37% greater bending stiffness in the vertical plane, while its flat faces provide natural mounting surfaces. Six 3510-class brushless motors (140 g each, 29.43 N thrust at full throttle on a 6S supply) drive 16-inch propellers. The total structural mass (excluding motors) is ~1001 g and the total frame-plus-motor mass is ~1841 g.

B. Material Selection

CFRP consists of high-strength carbon fibres embedded in an epoxy matrix, combining the tensile strength and stiffness of the fibres with the load-transfer capability of the matrix. Its exceptional strength-to-weight ratio, corrosion and fatigue resistance and dimensional stability make it ideal for drone frames. The frame was modelled as an orthotropic Epoxy Carbon UD laminate with $E_1 = 121$ GPa, $E_2 = 8.6$ GPa, $G_{12} = 4.7$ GPa, $\nu_{12} = 0.27$, $\rho = 1550$ kg/m^3 and a conservative design ultimate strength $\sigma_{UTS} = 1500$ MPa. A symmetric [0/+45/−45/90]s stacking sequence is adopted, in which 0° plies resist arm bending, ±45° plies resist motor-induced torsion and 90° plies improve transverse stiffness.

C. Design Calculations

The single-rotor disc area and total thrust are:

$$A = \pi D^2/4 = \pi(0.406)^2/4 = 0.1295\ m^2 \quad (1)$$

$$T_{total} = 6 \times (m \cdot g) = 6 \times 29.43 = 176.58\ N \quad (2)$$

The maximum bending moment at the arm root and the corresponding bending stress are:

$$M_{max} = T_{motor} \times L = 29.43 \times 400 = 11\,772\ N \cdot mm \quad (3)$$

$$\sigma_b = M \cdot y/I_x = (11\,772 \times 7.5)/4702 = 18.78\ MPa \quad (4)$$

The factor of safety and Von-Mises equivalent stress used as the failure criterion are:

$$FoS = \sigma_{UTS} / \sigma_{VM,max} \quad (5)$$

$$\sigma_{VM} = \sqrt{[(\sigma_1-\sigma_2)^2+(\sigma_2-\sigma_3)^2+(\sigma_3-\sigma_1)^2]/2} \quad (6)$$

A minimum FoS of 1.5, consistent with aerospace composite design practice, is adopted as the safety threshold. The thrust-to-weight ratio at a 17 kg maximum take-off weight is TWR = 176.58/(17×9.81) = 1.06.

D. FEA Setup and Boundary Conditions

Static structural analysis was performed in ANSYS Workbench. All six motor-mount surfaces were fully constrained (all six degrees of freedom), simulating the in-flight hover condition in which six propeller thrust forces react the payload, and four downward payload forces (25, 50, 75, 100 N) were applied to the lower face of the central plate (Fig. 2). The principal FEA parameters are summarised in Table I.

Fig. 2. Static structural boundary conditions: fixed supports at the six motor mounts (top) and the applied downward force at the hub (bottom).

Table I. ANSYS Workbench FEA Setup Parameters

Parameter	Setting / Value
Material model	Orthotropic: E_1=121, E_2=8.6, G_{12}=4.7 GPa, ν_{12}=0.27
Boundary condition	Fixed support at all 6 motor mounts (6 DOF)
Applied loads	25, 50, 75, 100 N (−Z on central plate)
Mesh size	2 mm global; 1 mm at arm-hub junctions
Total elements	≈ 1 050 000
Harmonic range	0–700 Hz, 100 N, 2% damping

E. Mesh Independence Study

Five progressively refined meshes were evaluated at the 100 N load. Variation across the meshes was below 2.4%; the selected ~1.05 million-element mesh (Fig. 3) lies within 0.7% of the finest reference mesh for both deformation and stress, satisfying the 1% convergence criterion (Table II).

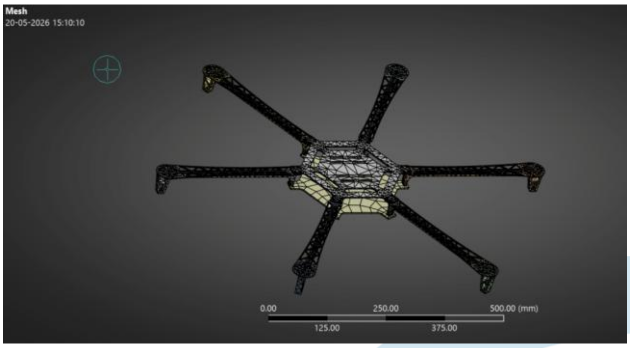

Fig. 3. Finite element mesh (~1.05 million elements) with local refinement at the arm-hub junctions.

Table II. Mesh Independence Study at 100 N

Mesh	Elements	Def. (mm)	Stress (MPa)	Dev.
1 Coarse	200 000	1.421	98.7	2.4%
2 Med.	450 000	1.403	97.1	1.2%
3 Selected	1 050 000	1.387	95.99	<0.7%
4 Fine	2 100 000	1.384	95.6	<0.4%
5 Finest	4 800 000	1.382	95.4	Ref.

IV. RESULTS AND DISCUSSION

A. Static Structural Analysis

Across all four load cases the frame responds in a linear-elastic manner, with the Von-Mises stress scaling linearly with load and the maximum stress consistently located at the arm-hub junctions (Table III). At the critical 100 N load (equivalent to a 10.19 kg payload) the maximum stress is 95.99 MPa, the maximum deformation is 1.387 mm — only 27.7% of the 5 mm rotor-disc tilt limit — and the FoS is 15.63, i.e. 10.4× the required minimum (Figs. 4 and 5).

Table III. Static FEA Results — CFRP Frame

Load (N)	Stress (MPa)	Def. (mm)	FoS	Status
25	23.998	0.347	62.51	Safe
50	47.997	0.694	31.25	Safe
75	71.995	1.041	20.84	Safe
100	95.994	1.387	15.63	Safe

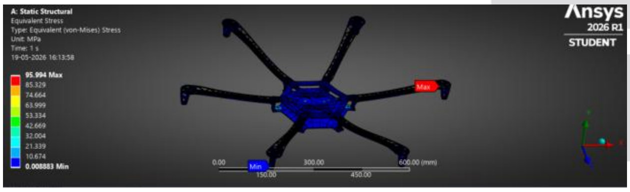

Fig. 4. Von-Mises stress distribution at 100 N (max 95.99 MPa at the arm-hub junction).

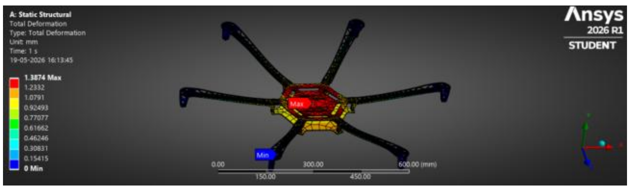

Fig. 5. Total deformation distribution at 100 N (max 1.387 mm at the central plate).

B. Material Comparison: CFRP vs Nylon 6/6

Because the Von-Mises stress depends only on geometry and load for linear-elastic analysis, both materials experience the same 95.99 MPa at 100 N, but the factor of safety differs dramatically with each material's strength (Table IV). Nylon 6/6 (σ_UTS = 80 MPa) fails at 100 N with FoS = 0.83 and is already unsafe at 75 N, whereas CFRP retains FoS = 15.63 and a sub-2 mm deformation against the ~62 mm estimated for nylon. This confirms the clear structural superiority of CFRP for heavy-lift UAV frames.

Table IV. Material Comparison at 100 N

Property	CFRP	Nylon 6/6
Young's modulus E_1	121 GPa	3.0 GPa
Tensile strength	1500 MPa	80 MPa
Max stress @ 100 N	95.99 MPa	95.99 MPa
Max deformation	1.387 mm	≈62.4 mm
FoS @ 100 N	15.63 (Safe)	0.83 (Fail)
Heavy-lift suitable	Yes	No

C. Modal Analysis

The first six natural frequencies of the CFRP frame range from 192.49 Hz to 687.81 Hz (Table V, Fig. 6). Mode 1 is a global bending mode of the arms and central body; Modes 2 and 3 (and 5 and 6) appear as near-identical pairs, reflecting the symmetric stiffness distribution of the six-arm geometry; Mode 4 is a radial arm mode. The fundamental frequency of 192.49 Hz lies well above the normal motor-excitation range, indicating high stiffness and low susceptibility to resonance.

Table V. Modal Analysis — Natural Frequencies

Mode	Freq. (Hz)	Mode	Freq. (Hz)
1	192.49	4	529.30
2	333.72	5	687.06
3	333.99	6	687.81

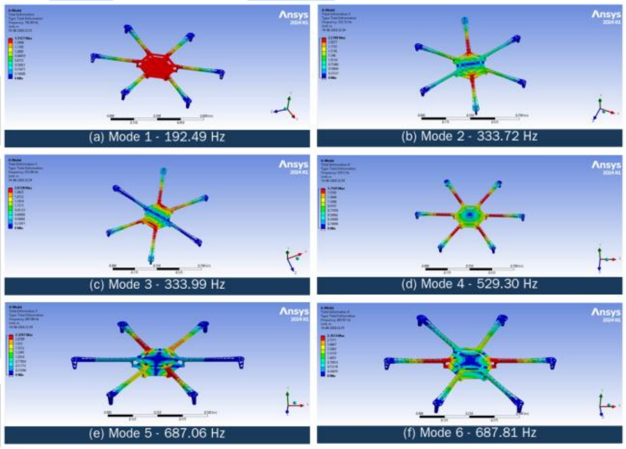

Fig. 6. First six mode shapes of the CFRP hexacopter frame.

D. Harmonic Response Analysis

Under a 100 N harmonic excitation swept over 0–700 Hz, resonance peaks occur near 192, 334 and 687 Hz, closely matching the modal results and confirming the dynamic model. The maximum equivalent stress over the range is 85.78 MPa and the maximum total deformation only 0.077 mm (Table VI). The frequency-response curves (Figs. 7 and 8) show that, between resonances, the response remains small and stable, indicating effective damping; the highest stresses again concentrate at the body-arm junctions while the arms remain lightly stressed.

Table VI. Harmonic Response Results

Parameter	Result
Frequency range / load	0–700 Hz / 100 N
Max total deformation	0.076991 mm
Max equivalent stress	85.78 MPa
Resonance frequencies	~192, 334, 687 Hz
Max FR stress amplitude	12.266 MPa

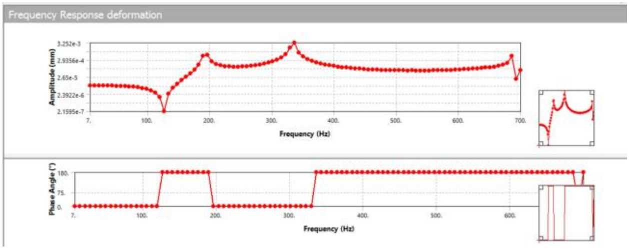

Fig. 7. Frequency response — total deformation amplitude vs frequency (0–700 Hz).

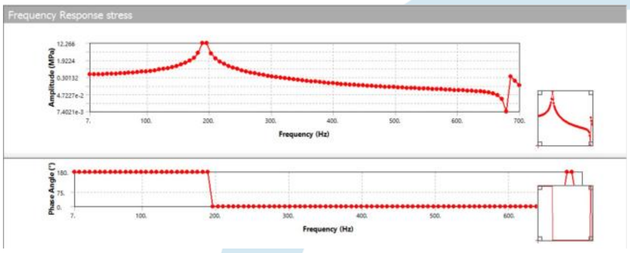

Fig. 8. Frequency response — equivalent stress amplitude vs frequency (0–700 Hz).

E. Explicit Dynamic (Impact) Analysis

Two explicit-dynamic analyses assessed the landing structure on contact with a rigid ground. A gravity-load settling case gave a maximum deformation of 0.41594 mm and a maximum stress of 2.2029 MPa. A more severe 1 m hard-drop case (impact velocity $v = \sqrt{2gh} = 4.43$ m/s) produced a peak Von-Mises stress of 385.84 MPa against the 1500 MPa CFRP strength, i.e. FoS = 3.89 (Table VII, Fig. 9). Although the total-deformation history peaked at 18.2 mm, a directional (Y-axis) analysis (Fig. 10) showed this to be almost entirely vertical rigid-body translation of the descending leg rather than elastic flexing, the true structural deformation remaining sub-millimetre. The 5 mm serviceability limit used for the in-flight static cases does not apply to an accidental hard landing, which is instead assessed against material strength; the FoS of 3.89 comfortably satisfies this. Modelling the full-vehicle landing case is identified as future work.

Table VII. Drop-Test (1 m Impact) Results

Parameter	Value
Drop height / velocity	1 m / 4.43 m/s
Peak Von-Mises stress	385.84 MPa
CFRP ultimate strength	1500 MPa
Factor of safety	3.89 (Safe)
True elastic deformation	Sub-millimetre

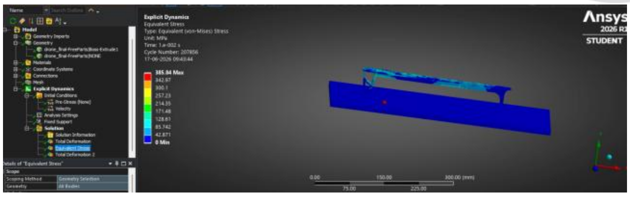

Fig. 9. Explicit-dynamic Von-Mises stress during the 1 m impact (max 385.84 MPa).

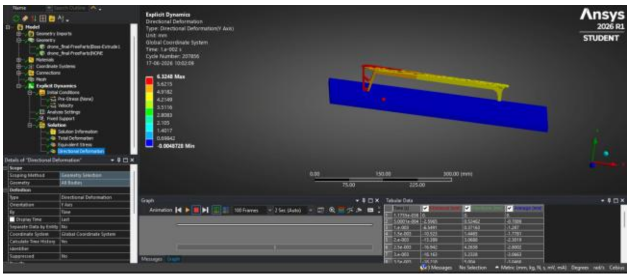

Fig. 10. Directional (Y-axis) deformation, confirming the large displacement is vertical rigid-body travel.

V. CONCLUSION

A CFRP heavy-lift hexacopter frame was designed in SolidWorks 2025 and validated through static, modal, harmonic and explicit-dynamic FEA in ANSYS Workbench. Static analysis showed a linear-elastic response with a maximum stress of 95.99 MPa, a deformation of 1.387 mm and FoS = 15.63 at the critical 100 N load, with the arm-hub junctions identified as the critical regions. A direct comparison demonstrated the superiority of CFRP, which remained safe where an identical Nylon 6/6 frame failed (FoS = 0.83). Modal analysis gave first six natural frequencies of 192.49–687.81 Hz, well above the motor-excitation range, and the harmonic analysis confirmed low deformation (0.077 mm) and moderate stress (85.78 MPa) with effective damping. The explicit-dynamic drop test confirmed survival of a 1 m hard landing with FoS = 3.89 and negligible permanent deformation. The proposed frame is therefore structurally safe, dynamically stable and impact-resistant, and is well suited to reliable heavy-lift UAV applications.

Future work includes topology optimisation of the arm-hub junction, experimental validation through prototyping and modal/strain testing, ply-level laminate modelling using ANSYS Composite Pre/Post, fatigue and full-vehicle drop analysis, and fluid–structure interaction studies incorporating aerodynamic and gust loads.

REFERENCES

[1] S. Raut, A. Jadhav and R. Jadhav, "Structural analysis and material comparison of carbon fibre and ABS for a hexacopter UAV frame under 3 kg payload," Int. J. Intelligent Unmanned Systems, vol. 12, no. 2, pp. 192–219, 2024.

[2] M. Gutierrez-Rivera et al., "Hexacopter CAD design, construction and FEA experimental validation for a 30 kg agricultural payload," Modelling, vol. 5, no. 3, pp. 1239–1267, 2024.

[3] A. Srivastav et al., "Comparative structural analysis of multi-rotor UAV configurations under payload and aerodynamic loading," J. Inst. Eng. (India): Series C, 2026.

[4] O. Bay and S. Eryıldız, "Topology-optimised drone frame design: 30% mass reduction while maintaining structural integrity," Gazi Univ. J. Sci. Part C, vol. 12, no. 2, pp. 427–437, 2024.

[5] Generative Design Research Group, "AI-driven generative design for agricultural hexacopter frame optimisation," Global J. Eng. Technol. Advances, vol. 24, no. 1, pp. 067–085, 2025.

[6] K. Vijayalakshmi et al., "Fluid–structure interaction analysis of a multi-rotor UAV with 140 material combinations for a 25 kg payload," Rev. Adv. Mater. Sci., vol. 62, no. 1, 2023.

[7] M. Karpenko et al., "Multi-objective genetic algorithm optimisation of a composite UAV wing shell," Drones, vol. 9, no. 2, art. 99, 2025.

[8] A. Kubit et al., "Autoclave vs vacuum-bag CFRP manufacturing: autoclave achieves 1088 MPa bending strength," Materials, vol. 18, no. 1, art. 102, 2025.

[9] A. Arkuszyńska and M. Rośkowicz, "Fatigue life of CFRP bolted joints at elevated temperatures," Polymers, vol. 18, no. 2, art. 182, 2026.

[10] W. Chen, X. Meng, Y. Wang, H. Liu and J. Lu, "Experimental structural vibration testing of large multi-rotor drone arms," Int. J. Micro Air Vehicles, vol. 15, 2023.

[11] Y. Zhong, H. Wang, L. Kong and D. Chen, "Three-stage fatigue damage progression in off-axis CFRP composites under cyclic loading using DIC," Heliyon, vol. 10, no. 4, art. e25577, 2024.

[12] G. Ferretti et al., "ACP-based ply-level FEA of UAV composite wing structural dynamics," Simul. Model. Pract. Theory, vol. 141, art. 103099, 2025.

[13] I. Sarić et al., "Hexacopter design, structural analysis and FEA validation," New Technologies, Development & Application IV, pp. 74–81, 2021.

[14] H. Li et al., "Carbon-fibre prepreg-reinforced composites: complete mechanical properties and manufacturing characterisation," Polymers, vol. 18, no. 11, 2025.